Electronic Supplementary Information

Activating Co nanoparticles on graphitic carbon nitride *via* tuning the Schottky barrier by P doping for the efficient dehydrogenation of ammonia-borane

Shao-Hong Xu, [a] Jing-Feng Wang, *[b,c] Alexsandra Valério, [d] Wen-Yu Zhang, [a] Jia-Lun Sun, [a] and Dan-Nong He *[a,b]

[a] School of Materials Science and Engineering, Shanghai Jiao Tong University, 800 Dongchuan Road Shanghai 200240, P. R. China. E-mail:

[b] National Engineering Research Center for Nanotechnology, 28 East Jiangchuan Road, Min Hang District, Shanghai 200241, P.R. China. E-mail:

[c] Shanghai University of Medicine & Health Sciences, 279 Zhouzhu highway, Shanghai, 201318, P. R. China.

[d] Department of Chemical Engineering and Food Engineering, Federal University of Santa Catarina, 88040-900 Florianópolis, SC, Brazil.

Corresponding author e-mail address: hdn_nercn@163.com; jfwang@shu.edu.cn.

Table of content

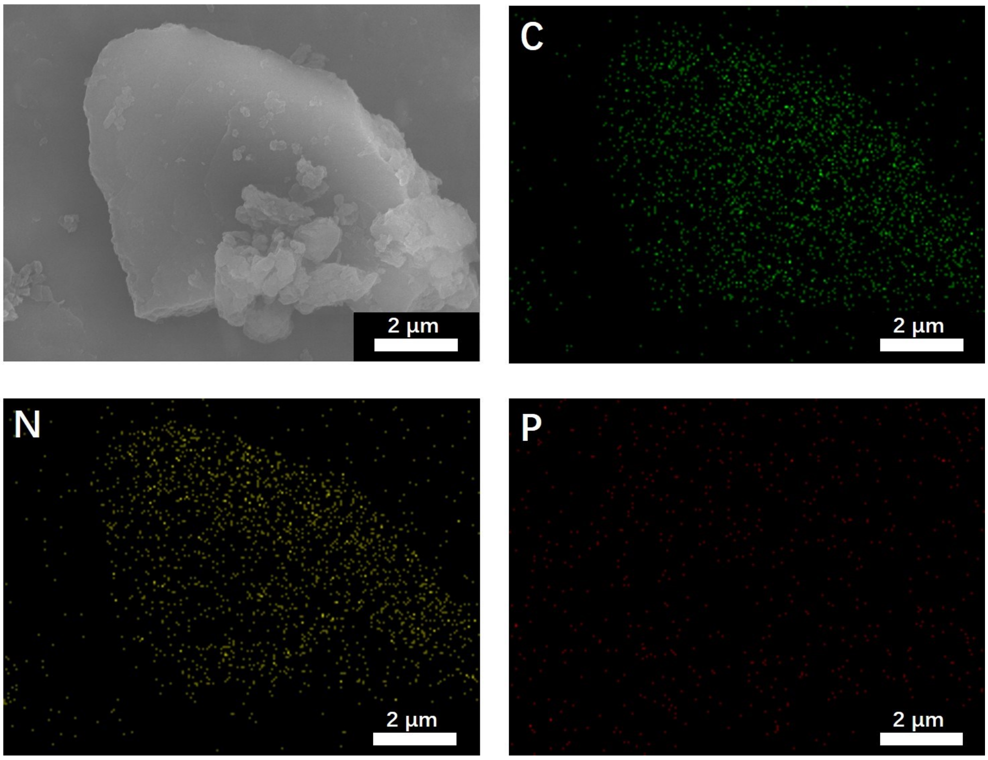

Fig. S1 EDS elemental mapping images of P_0CN.

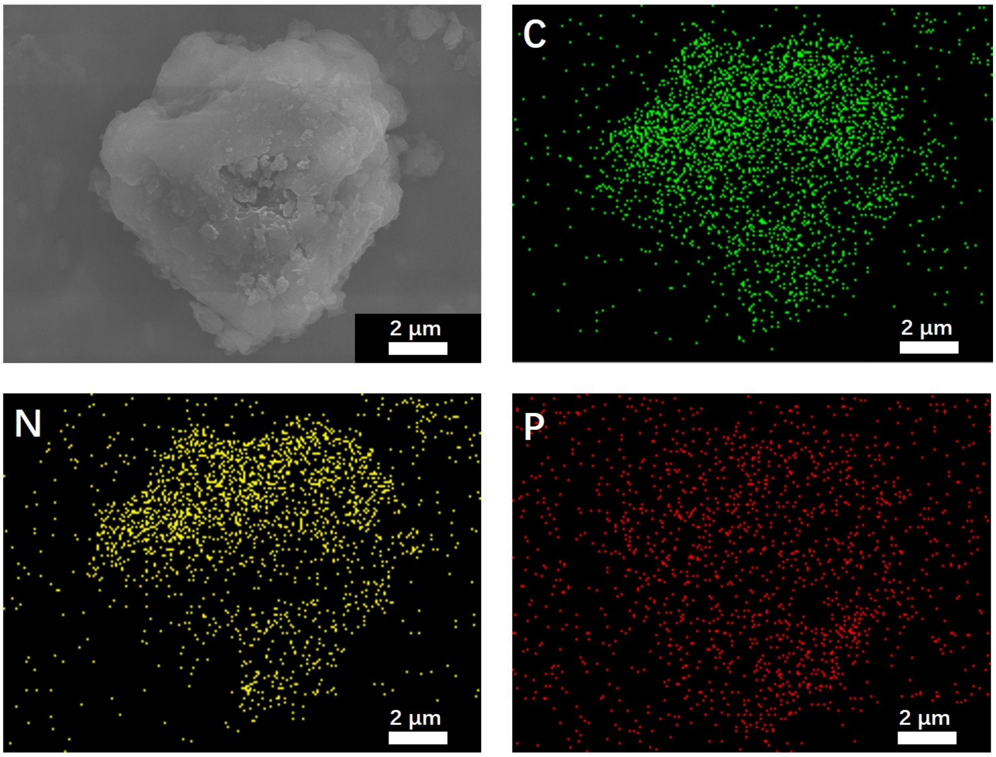

Fig. S2 EDS elemental mapping images of $P_{3.59}CN$.

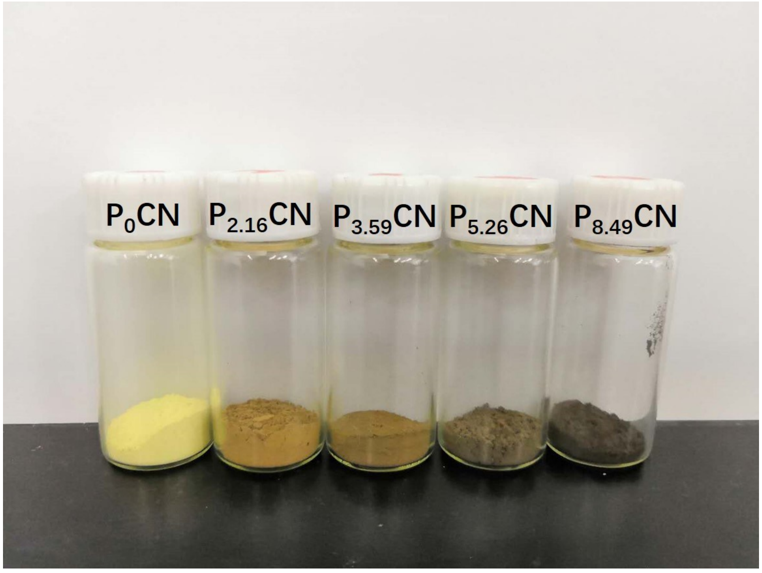

Fig. S3 Photographs of P_0CN, $P_{2.16}$CN, $P_{3.59}$CN, $P_{5.26}$CN, and $P_{8.49}$CN. It is shown a significant color change from pale yellow to black for the samples.

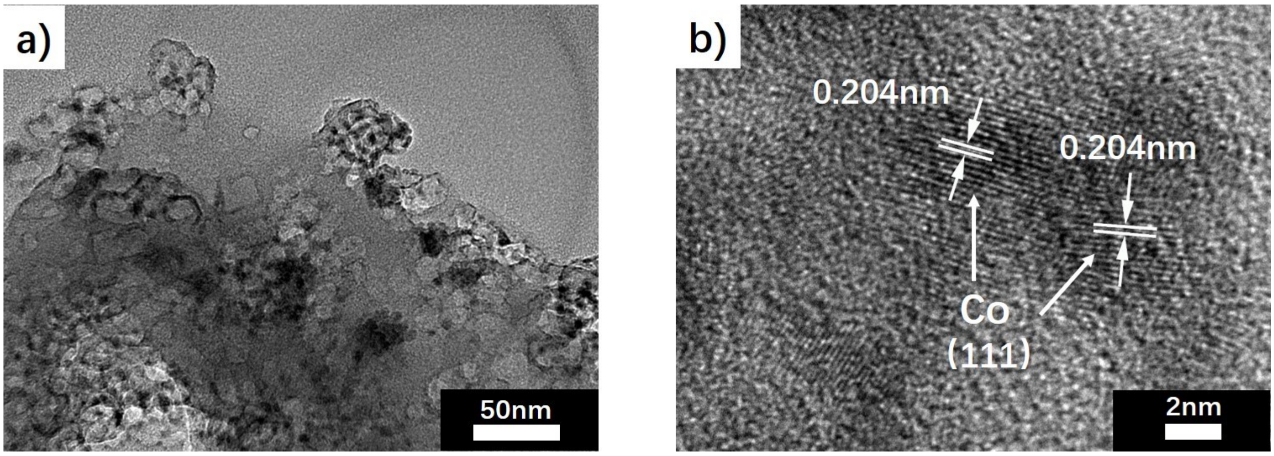

Fig. S4 Typical TEM (a) and HRTEM (b) images of $Co/P_{3.59}CN$. The interlayer space of 0.204 nm in $Co/P_{3.59}CN$ is ascribed to the (111) lattice plane of metallic cobalt nanocrystal.

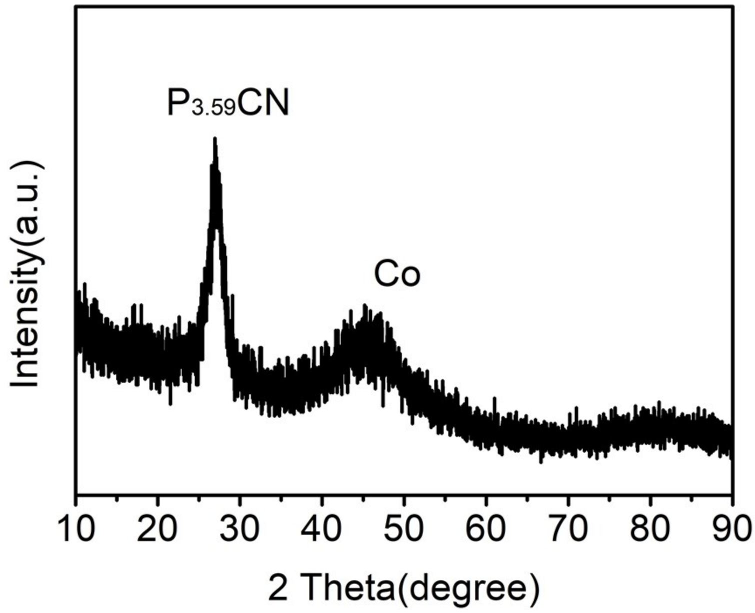

Fig. S5 XRD pattern of Co/$P_{3.59}CN$. When Co NPs are introduced into $P_{3.59}CN$, a weak and broad peak located at 44.2° is observed, indicating the formation of metallic Co NPs. The diffraction peak located at 27.3° which corresponds to $P_{3.59}CN$ exhibits no obvious change after the loading of Co NPs.

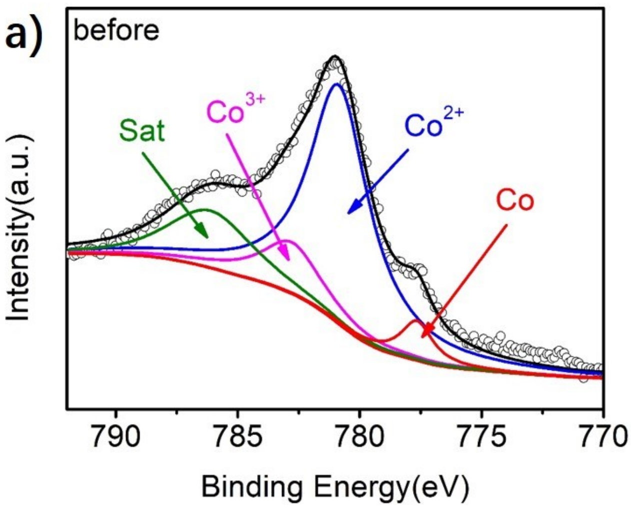

Fig. S6 Co2p deconvoluted XPS spectra of Co/$P_{3.59}$CN before (a) and after (b) etching treatment. The peak of metallic Co is obviously enhanced after etching, indicating that metallic Co NPs are existed under the oxidation layer.

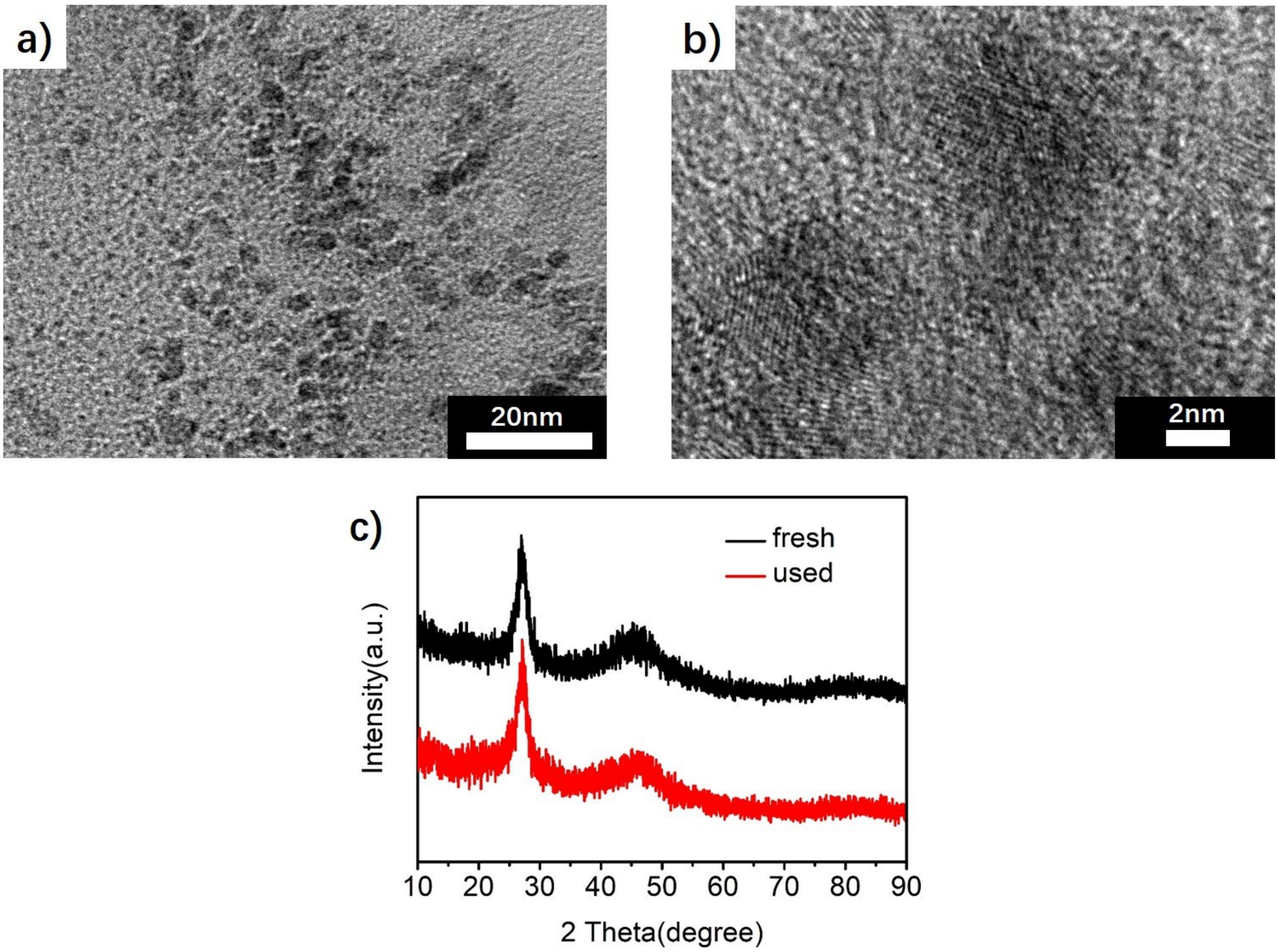

Fig. S7 Typical TEM (a-b) images of Co/$P_{3.59}$CN catalysts after eight cycles and XRD patterns(c) of fresh and used Co/$P_{3.59}$CN catalysts. No obvious change was found in the Co/$P_{3.59}$CN catalysts after eifht cycles, indicating the good stability of Co/$P_{3.59}$CN.

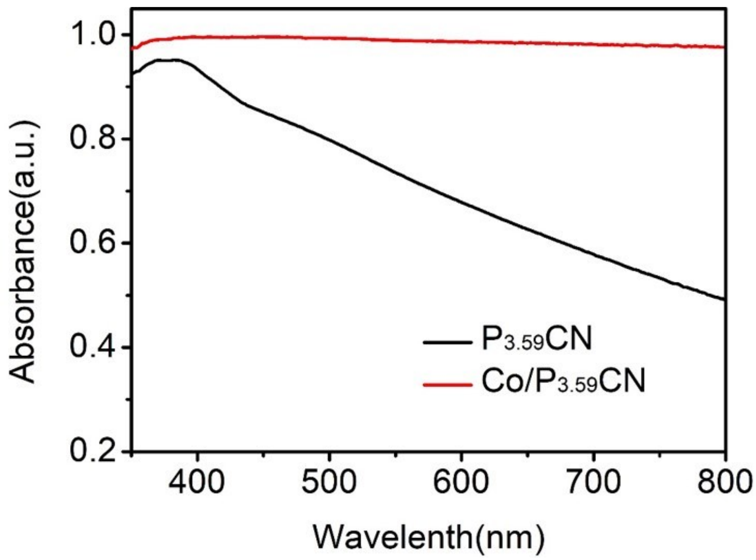

Fig. S8 UV/Vis diffuse reflection spectra of $P_{3.59}CN$ and $Co/P_{3.59}CN$.

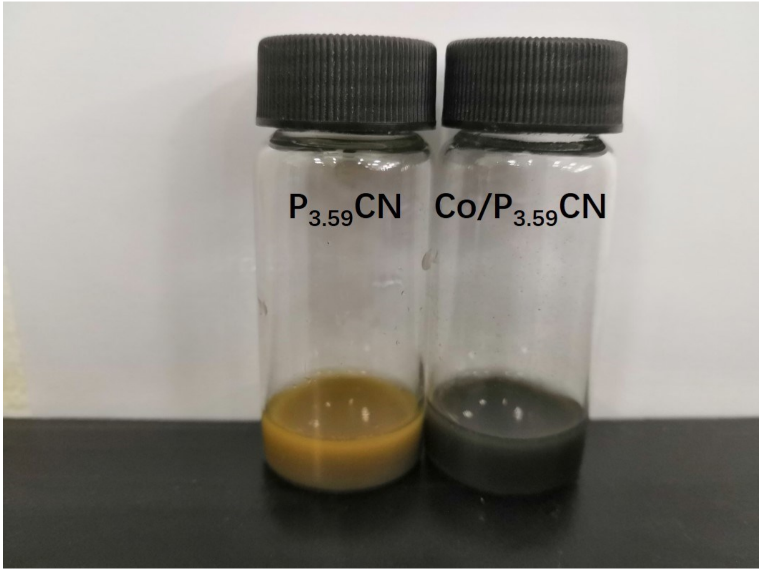

Fig. S9 Photographs of $P_{3.59}CN$ and $Co/P_{3.59}CN$.

Table S1 The P atomic percentage of P_0CN, $P_{2.16}CN$, $P_{3.59}CN$, $P_{5.26}CN$, and $P_{8.49}CN$.

Samples	HEDP amount (g)	P (%)
P_0CN	0	0
$P_{2.16}CN$	0.2	2.16
$P_{3.59}CN$	0.4	3.59
$P_{5.26}CN$	0.6	5.26
$P_{8.49}CN$	0.8	8.49